CHAPTETER V

FABRICATION OF DENDRIMER POROGEN-CAPSULATED MESOPOROUS SILICA VIA SOL-GEL PROCESS OF SILATRANE PRECURSOR

5.1 Abstract

Mesoporous silica materials with ordered structures were prepared from a silatrane precursor and a poly(amido amine) dendrimer porogen under the dilute acidic condition via the sol-gel process. With decreasing the concentration of the dendrimer and adding much water, the production of undesirable amorphous silica was diminished and spherical particles with smooth surface became in majority. Two arrays were fabricated in the silica particles. Although pore diameters were within sizes of shrank and extended dendrimers, center-to-center distance of template pores was different between two arrays, and the difference was close to a molecular length of silatrane. This indicates that one molecule of silatrane constructed polysiloxane walls in the first array and origomeric silatrane formed walls in the second array. It was referred that the intrinsic (hydrogen bonding) characters of the hydrolyzed silatrane resulted in hydrogen bonded oligomers and reinforced the hydrogen bonding interaction with dendrimer porogen as well as electrostatic interaction, giving rise to two types of template arrays.

5.2 Introduction

A new generation of mesoporous materials has been attractive during more than the past 10 years. In many studies, tetraethyl orthosilicate (TEOS) was used as a silica source for the syntheses of various silica mesoporous materials such as the M41S family (MCM-41, MCM-48 and MCM-50), and the formation mechanisms with surfactants as templates under acidic or basic condition were discussed [1-12]. However, a new silica source, silatrane, was introduced in place of it. Silatrane is an organosilicate that has been become a great interest for the past few years to produce

advanced materials, especially mesoporous materials via sol-gel process [13, 14]. Wongkasemjit and her coworkers [15-23] have synthesized highly pure silatrane via the "Oxide One Pot Synthesis" process for producing mesoporous materials through the sol-gel process. The reaction of silatrane precursor with different surfactant templates provided variety of highly quality products, denoted by MFI, ZSM-5, and MCM-41 [16,17,22]. In addition, the products have not only high surface area but also high ordering. However, when this method was applied for synthesis of SBA-1 cubic mesoporous silica, three-dimensionally ordered mesopores were invariably produced at different surfactant concentrations and reaction temperatures [24].

The inclusion of guest molecules in mesoporous materials is one of focused subjects. Some efforts have been made to incorporate aluminum or other atoms such as V, Mo, Co, Fe and Ti into mesoporous silica materials by using silatrane as a precursor, and the products with catalytic functionality were named by TS-1, Ti-MCM-41, Mo-MCM-41, VS-1 and Fe-MFI [18-21,23]. Dendritic guest molecules (poly(propyleneimine) dendrimers) containing amidoferrocenyl moieties were also incorporated into a mesoporous silica hosts (MCM-41) with highly ordered channels [25]. This is a novel type of redox-active materials. Meanwhile, poly(propyleneimine) tetrahexacontaamine dendrimers (DAB-Am-64) was used as a single molecule template to produce mesoporous silica from TEOS [26]. X-ray diffraction (XRD) patterns revealed the occurrence of mesoporous silica but transmission electron microscopic (TEM) analysis of a stained product showed the images of "globular" and "disordered filaments". The 4.0^{th} generation (G4) poly(amido amine) (PAMAM) dendrimer was also used as a template for the sol-gel reaction of TEOS [27].

Later, PAMAM dendrimer-templated, TEOS-based mesoporous silica was characterized by TEM [28]. After the removal of dendrimers by calcination, nanopores were disorderly maintained in the silica matrix. A PAMAM dendrimer was also utilized as a single molecule template to synthesize nanopores in iron phosphate mesoporous materials [29]. Although TEM images confirmed the formation of hexagonal ordering of nanopores, well-defined ordering at wide domains was not found.

In the present work, silica gel was synthesized by using a silatrane precursor and a G4 PAMAM dendrimer porogen instead of a surfactant template. Since silatrane and dendrimer are both water soluble, the experiments were thoroughly carried out in aqueous medium. The ordered morphology and template array were determined by electron microscopy. This research is a report on the formation of ordered mesoporous silica capsulating dendrimer porogen.

5.3 Experimental

5.3.1 Materials

Fumed silica (SiO_2, 99.8%) (Sigma-Aldrich), triethanolamine (TEA) (Carlo Erba), ethylene glycol (J.T.Baker, USA), acetronitrile (Labscan, Asia), amine-terminated G4 PAMAM dendrimer (Aldrich), H_2SO_4 (Labscan, Asia) and NaOH (Labscan, Asia) were used without treatment.

5.3.2 Synthesis of silatrane precursor

Silatrane precursor ($N(CH_2CH_2O)_3SiOCH_2CH_2N(CH_2CH_2OH)_2$, Scheme 1) was synthesized from a mixture of SiO_2 and TEA in ethylene glycol via the Oxide One Pot Synthesis process [13,14]. The reaction was taken place at a boiling point (200 °C) of ethylene glycol under a nitrogen atmosphere. It was completed within 10 h, and the remaining ethylene glycol was removed under vacuum at 110 °C. The crude brown solid was washed with acetonitrile to remove unreacted TEA and ethylene glycol. The white silatrane products were dried in a vacuum desiccator overnight prior to be characterized.

5.3.3 Synthesis of mesoporous silica

Silatrane (1.4 g, 5 mmol) was suspended in a solution of 0.3 M H_2SO_4 (14 cm^3), and a solution of NaOH (0.068 g, 1.7 mmol) was added to the suspension. After stirring for 0.5 h, required amount of dendrimer was added to the suspension

under vigorous stirring. After 0, 10 or 30 cm^3 of water was added, the mixture was stirred for 4 h and allowed to age for 5 days at room temperature. The white precipitates were filtered, washed with water, and dried overnight in the atmosphere (without removed the template). The products labeled DnH0 (n = 1-4) were synthesized via four concentrations of dendrimer at 1.41, 2.81, 4.22 and 5.64 mM, respectively. The products added 10 and 30 cm^3 of water were denoted DnH10 and DnH30 (n = 1 – 4), respectively.

5.3.4 Measurements

The precursor and the products were characterized by Fourier transform infrared (FT-IR) absorption spectra, which were recorded on a Nicolet 6700 FT-IS spectrometer, using KBr discs. The thermogravimetric analysis was carried out on a Seiko EXSTAR 6000 TG/DTA analyzer. Using 300 cm^3/min airflow, the temperature was raised to 700 °C at a constant rate of 5 °C/min. Morphology and particle size of the products were analyzed using a XL-30ESEM scanning electron microscope (SEM), operating at 30 kV. The observations of TEM images were performed with a Hitachi H-7000 instrument at an accelerating voltage of 100 kV. Prior to the TEM observation, a small amount of product was sonicated in methanol for 10 min with a Branson 1510 instrument, and then a drop of the dispersion was dried on a holey carbon grid at room temperature. Powder XRD patterns were measured on an X-ray diffractometer (D8 ADVANCE, Bruker AXS) using CuK_α (λ = 0.154 nm) radiation in 2θ range of 1.5 - 10° with a step of 0.02 °/s.

5.4 Results and discussion

Mesoporous silica was produced from silatrane precursor by using G4 PAMAM dendrimer as a porogen. Preparation conditions of silica were listed in Table 5.1. In the FT-IR adsorption spectrum of silatrane precursor (Figure 5.1), there were characteristic vibration bands at 3400-3300 (m, νOH), 2986-2860 (m, νCH_2), 1093, 1073, 785 and 729 cm^{-1} (s, νSi-O, νSi-O-C and νC-O). On the other hand, the

IR absorption spectra of the silica products (DnH0) including dendrimer porogens were fairly different from that of the precursor, as compared in Figure 5.1. The OH stretching band at ~3400 cm^{-1} was intensified in comparison with the CH_2 stretching bands, indicating the formation of OH groups as a result of hydrolysis of alkoxy group in the precursor. Moreover, bands at 785 and 729 cm^{-1} disappeared, and new bands were observed at 1200, 970 and 795 cm^{-1}, which were attributed to the formation of Si-O-Si bands. These variations confirm the sol-gel reaction of silatraine. Additionally, amide I and II bands were observed at 1651 and 1553 cm^{-1}, respectively, suggesting the coexistence of PAMAM dendrimer in the composite materials. When the dendrimer content was increased, the intensity of IR bands attributing to silica decreased relatively in comparison with amide bands. Similar IR spectra and tendency were observed even for DnH30 products. This means that the incorporation of dendrimers depends on the supplied amount.

A TGA curve of the silatrane precursor exhibited only one-step transition of weight loss at around 370°C, corresponding to the decomposition of organic component [17,19,20,22]. On the other hand, the decomposition of dendrimer occurred at temperature above 200 °C, but the oxidation of dendrimers and the decomposition of oxidized dendrimers additionally proceeded up to 700 °C. A TGA curve of the product D2H0 was superposition of those of silatrane and dendrimer, that is, it resulting consists of three steps, as seen in Figure 5.2. This means the reasonable incorporation of dendrimers in the silica particles. The similar multistep decomposition was observed for silica materials prepared by using amine-terminated templates [30].

Morphologies of the products, which were prepared at different conditions, were compared in SEM images, as represented in Figure 5.3. The images displayed spherical particles with smooth surface and diameter in the range of 2 – 5 μm. With increasing the concentration of dendrimer, amount of amorphous silica slightly increased. Interestingly, when water was added into the reaction mixture, the rate of condensation polymerization slowed down.

TEM images of the silica products are shown in Figure 5.4. All images present ordered pattern of the hexagonal array. Very importantly, it was for the first

time so far as we know that these ordered mesoporous silica materials were successfully prepared by using dendrimer porogen. Although the preparation of dendrimer-incorporated mesoporous silica has been performed, no report showed TEM images of wide-range ordered array [25-27]. It must be also noted that the TEM images showed two kinds of crystal arrays with different unit lattice. The short- and long-spacing arrays were found in the different silica products, in the different sampling from same product and even in the same sampling of the same product, indicating the coexistence of two arrays, which were denoted by array S and L.

The pore sizes (φ_{pore}) (3.7 – 4.9 nm for array S, 5.9 – 6.8 nm for array L) observed is within the size region of G4 PAMAM dendrimer, because the dendrimer size is variable depending on the condition. The standard size was 4.0 ~ 4.5 nm [29]. The center-to-center distance a_0 of pores in two arrays are listed in Table 5.1. This distance (4.2 – 7.0 nm for array S, 9.4 – 11.0 nm for array L) was fairly different between two arrays. However, as it was clear from Table 5.1, even if the concentration of dendrimer increased and the reaction mixture was diluted, the arrangement of arrays was not seriously changed.

XRD patterns of the products are shown in Figure 5.5. Broad Bragg peaks were observed at low 2θ reflection, indicating the ordered mesoporous silica. The 2θ values for all products were listed in Table 5.1, which also includes the spacing values (d values) calculated from a Bragg equation and the a_0 values calculated from d values. The spacing (3.84 - 4.32 nm) of the low angle reflection (2.04 - 2.30°) can be assigned to a [100] plane of hexagonal array, because it is closely similar to the distance (3.7 – 6.1 nm) of [100] plane from TEM. Correspondingly, both a_0 values from XRD and TEM were consistent. Since the spacing of a Bragg peak at a high 2θ value is almost half of the [100] plane, this spacing corresponds to the [200] plane. The d values of [100] and [200] planes or the a_0 values were independent of the concentrations of dendrimer and reaction mixture in consistency with the behavior of the a_0 values from TEM.

Crystal arrays in dendrimer-incorporated mesoporous materials previously reported [26-30] is compared to the present array in Table 5.2. While the d values of a [100] space obtained from XRD for PAMAM dendrimer-incorporated mesoporous materials are commonly close and independent of precursor materials, those are

larger than the value for DAB-Am-64-incorporated silica. This is due to the difference of dendrimer size. Incidentally, the hydrodynamic diameter of soft-core DAB-Am-64 is 3.96 nm and the diameter at dense-core limit is predicted to be ~2.50 nm [26]. On the other hand, the diameter of G4 PAMAM dendrimer was calculated as 4.0 nm and evaluated to be ~ 4.5 nm in solution [31]. The a_0 values (4.9 and 4.4 – 5.0 nm, respectively), which were calculated from a [100] space of PAMAM dendrimer-incorporated mesoporous materials prepared from $FePO_4$ and silatrane precursors, were consistent with the values from TEM, and the pore sizes in both mesoporous materials were reasonably identified with porogen size.

The formation of mesoporous materials from inorganic precursor and charged surfactant template is driven by the electrostatic interaction [2]. Additionally, in the present case where ionic dendrimer was used as a template instead of conventional ionic surfactant, hydrogen bonding interaction between amide (and amine) groups of dendrimer and hydroxyl groups of hydrolyzed silatrane is possible as a driving force for the construction of mesopores besides electrostatic interaction (Scheme 5.1). Such interaction of precursor with porogen molecule is stimulated at high dendrimer concentration or in the concentrated reaction mixture, but the precipitation of composites occurs competitively with the formation of mesoporous silica. Therefore, dilute condition of dendrimer and reaction mixture is preferable to prepare the ingenious mesoporous materials such as spheres with smooth surface, as noticed from SEM results. It can be noted that the slow sol-gel reaction in the dilute solution is evocative the formation of well-aged silica particles.

Most important notification is that the second crystal array (L) was found in the PAMAM dendrimer-incorporated mesoporous silica from silatrane precursor. Since calculated molecular length of silatrane is ~1.4 nm, the a_0 value of ~5.9 nm can be estimated, if the dendriemr size is 4.5 nm. The a_0 value of array S coincides with this value, but that of array L does. Figure 5.6 illustrates the CPK models of silatrane, silatrane oligomers, and G4 PAMAM dendrimer. The observed a_0 value of array L is reasonable, if silatrane oligomers (probably trimer or tetramer) interpose and form polysiloxane walls between dendrimer porogens (see scheme 5.1). Such oligomer formation is possible by hydrogen bonding between hydroxyl groups in hydrolyzed

silatrane but does not occur on TEOS and $FePO_4$ precursor. The hydrogen bonding characters of the hydrolyzed silatrane will reinforce the hydrogen bonding interaction with dendrimer porogen as well as electrostatic interaction.

5.5 Conclusions

Mesoporous silica materials have been successfully synthesized by using silatrane as a silica source and G4 PAMAM dendrimer as a porogen under the dilute acidic condition via the sol-gel process. At the optimum conditions, spherical particles with smooth surface were obtained. The ordered crystal arrays were observed in TEM images. This is the first report for the TEM images of dendrimer-incorporated mesoporous silica with ordered array, as far as we know. Noticeable topic is that two kinds of crystal arrays were created in the mesoporous silica. One array is same as the ordered structure from conventional dendrimer-incorporated mesostructures, but the other one is intermediated by oligomers of hydrolyzed silatrane, which are interacted by hydrogen bonding between hydroxyl groups on hydrolyzed silatrane. This unique character of hydrolyzed silatrane also acts for the hydrogen bonding interaction with dendrimer porogen and give rise to the strict ordering of nanopores. The dendrimer-incorporated mesoporous materials are useful for applications like catalysis, molecular segregation and so on, because dendrimers have enough void volumes in the internal to include guest molecules.

5.6 Acknowledgements

This research was financially supported by the Thailand Research Fund (TRF), the Postgraduate Education and Research Program in Petroleum and Petrochemical Technology (ADB) Fund, and the Ratchadapisake Sompote Fund, Chulalongkorn University.

5.7 References

1. J.S. Beck, J.C. Vartuli, W.J. Roth, M.E. Leonowicz, C.T. Kresge, K.T. Schmitt, C.T-W. Chu, D.H. Olson, E.W. Sheppard, S.B. McCullen, J.B. Higgins, and J.L. Schlenker, *J. Am. Chem. Soc.* 1992, 114, 10834-10843.
2. Q. Huo, D.I. Margolese, D.I. Ciesla, D.G. Demuth, P. Feng, T.E. Gier, P. Sieger, A. Firouzi, B.F. Chemelka, F. Schu¨ th, and G.D. Stucky, *Chem. Mater.* 1994, 6, 1176-1191.
3. J.S. Beck, J.C. Vartuli, G.J. Kennedy, C.T. Kresge, W.J. Roth, and S.E. Schramm, *Chem. Mater.* 1994, 6, 1816-1821.
4. Q. Huo, D.I. Margolese, U. Ciesla, D.G. Demuth, P. Feng, T.E. Gier, P. Sieger, A. Firouzi, B.F. Chemelka, and G.D. Stucky, *Chem. Mater.* 1996, 8, 1147-1160.
5. T.P. Tanev and T.J. Pinnavaia, *Chem. Mater.* 1996, 8, 2068-2979.
6. W. Zhang, T.R. Pauly, and T.J. Pinnavaia*Chem. Mater.* 1997, 9, 2491-2498.
7. M.S. Morey, A. Davidson and G.D. Stucky, *J. Porous. Mater.* 1998, 5, 195-204.
8. L. Huang, W. Guo, P. Deng, Z. Xue, and Q. Li, *J. Phys. Chem. B* 2000, 104, 2817-2823.
9. T.R. Pauly, and T.J. Pinnavaia, *Chem. Mater.* 2001, 13, 987-993.
10. A. Sayari, and S. Hamoudi, *Chem. Mater.* 2001, 13, 3151-3168.
11. Z. Yuan, and W. Zhou, *Chem. Phys. Lett.* 2001, 333, 427-431.
12. B. Smarsly, S. Polarz, and M. Antonietti, *J. Phys. Chem. B* 2001, 105, 10473-10483.
13. V. Jitchum, C. Sun, S. Wongkasemjit and H. Ishida, *Tetrahedron*, 2001, 57, 3997-4003.
14. W. Charoenpinijkarn, M. Suwankruhasn, B. Kesapabutr, S. Wongkasemjit, and A.M. Jamieson, *Eur. Polym. J.* 2001, 37, 1441-1448.
15. M. Sathupanya, E. Gulari, and S. Wongkasemjit, *J. Euro. Ceram. Soc.* 2003, 23, 1293-1303.
16. N. Phonthammachai, T. Chairassameewong, E. Gulari, A.M. Jameison, and S. Wongkasemjit, *J. Met. Mater. Min.* 2003, 12, 23.
17. P. Phiriyawirut, R. Magaraphan, A. M. Jamieson and S. Wongkasemjit, *Mater. Sci. & Eng. A* 2003, 361, 147-154.

18. P. Phiriyawirut, A.M. Jamieson, and S. Wongkasemjit, *Micropor. Mesopore. Mater.* 2005, 77, 203-213.
19. N. Thanabodeekij, W. Tanglumlert, E. Gulari, and S. Wongkasemjit, *Appli. Organomet. Chem.* 2005, 19 ,1047-1054.
20. N. Kritchayanon, N. Thanabodeekij, S. Jitkarnka, A. M. Jamieson, and S. Wongkasemjit, *Appli. Organomet. Chem.* 2005, 20, 155-160.
21. N. Phonthammachai, M. Krissanasaeranee, E. Gulari, A.M. Jamieson and S. Wongkasemjit, *Mater. Chem. Phys.* 2006, 97, 458-467.
22. N. Thanabodeekij, S. Sadthayanon, E. Gulari,and S. Wongkasemjit, *Mater. Chem. Phys.* 2006, 98, 131-137.
23. N. Thanabodeekij, E. Gulari and S. Wongkasemjit, *Powder Tech.* 2007, 173, 211-216.
24. W. tanglumlord, T. Imae, T. J. White, and S. Wongkasemjit, *J. Am. Ceram. Soc.*, 2007, 90, 3992-3997.
25. I. Diaz, B. Garcia, B. Alonso, C. M. Casado, M. Moran, J. Losada, and J. P-Pariente, *Chem. Mater.* 2003, 15, 1073-1079.
26. G. Larsen, E. Lotero, and M. Marquez, *Chem. Mater.* 2000, 12, 1513-1515.
27. G. Larsen, and E. Lotero, *J. Phys. Chem. B* 2000, 104, 4840-4843.
28. A. Mitra, A. Bhaumik, and T. Imae, *J. Nanosci. Nanotechol.* 2004, 14, 1052-1055.
29. X. Luo, and T. Imae, *Chem. Lett.* 2005, 34, 1132-1133.
30. J. Hukkamaki, and T. Pakkanen, *Micropor. Mesopore. Mater.* 2003, 65, 189-196.
31. A. D. Tomalia, A. M. Naylor, and W. A. Goddard III, *Angew. Chem. Int. Ed. Engl.* 1990, 29, 138.

Table 5.1. TEM and XRD data for crystal arrays in dendrimer-incorporated mesoporous silica

Sample			Array S (TEM)		Array L (TEM)		Space (XRD)	
Product	Dendrimer (g)	Added Water (cm^3)	φ_{pore} (nm)	a_0 (nm)	φ_{pore} (nm)	a_0 (nm)	$d_{[100]}$ (nm) (angle (degree))	$d_{[200]}$ (nm) (angle (degree))
D1H0	0.2	0				10.22	3.97(2.22)	
D2 H0	0.4	0			6.76	9.37	4.01(2.20)	
D2H10	0.4	10				9.36	4.05(2.18)	
D2H30	0.4	30	4.82	5.57			4.09(2.16)	1.91(4.62)
D3H0	0.6	0		5.65		11.00	4.08(2.16)	
D3H10	0.6	10	4.88	7.03			4.09(2.16)	1.85(4.76)
D3H30	0.6	30	3.66	4.23			4.32(2.04)	2.02(4.36)
D4H0	0.8	0		6.56	5.88	9.45	4.03(2.19)	1.97(4.48)
D4H10	0.8	10		4.93			3.84(2.30)	2.08(4.24)
D4H30	0.8	30		4.90			4.02(2.19)	2.08(4.25)

Table 5.2. Comparison of crystal arrays in dendrimer-incorporated mesoporous materials[a)]

Precursor/template (porogen)	$d_{[100]}$ (nm) (angle (degree)) (XRD)	a_0 (nm) (TEM)	φ_{pore} (nm) (TEM)	Reference
TEOS/DAB-Am-64	(3.25)(as) 2.5(3.5)(cal)			26
TEOS/PAMAM dendrimer	(2.5)(as) 3.2(2.7)(cal)			27
TEOS/PAMAM dendrimer	3.8(2.3)(cal)		3.9(cal)[b)]	28
TEOS/PAMAM dendrimer	4.0(2.2)(cal)			30
$FePO_4$/PAMAM dendrimer	4.2(2.1)(as) 3.8(2.3)(cal)	5.1(as)	3.2(as)	29
Silatrane/PAMAM dendrimer	3.8-4.3 (2.0-2.3)(as)	4.2-7.0(as) 9.4-11.0(as)	3.7-4.9(as) 5.9-6.8(as)	present

a) as; as-prepared, cal; calcinated.

b) Calculated from nitrogen adsorption data.

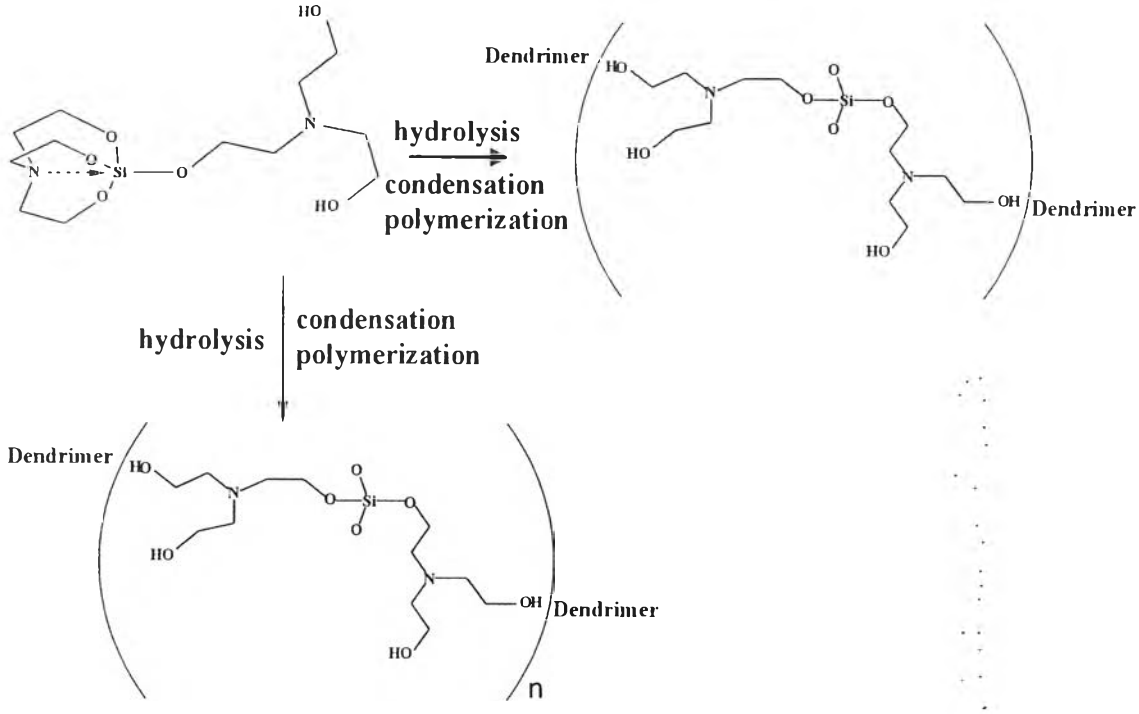

Scheme 5.1 The chemical structures of silatrane and the products of sol-gel reaction.

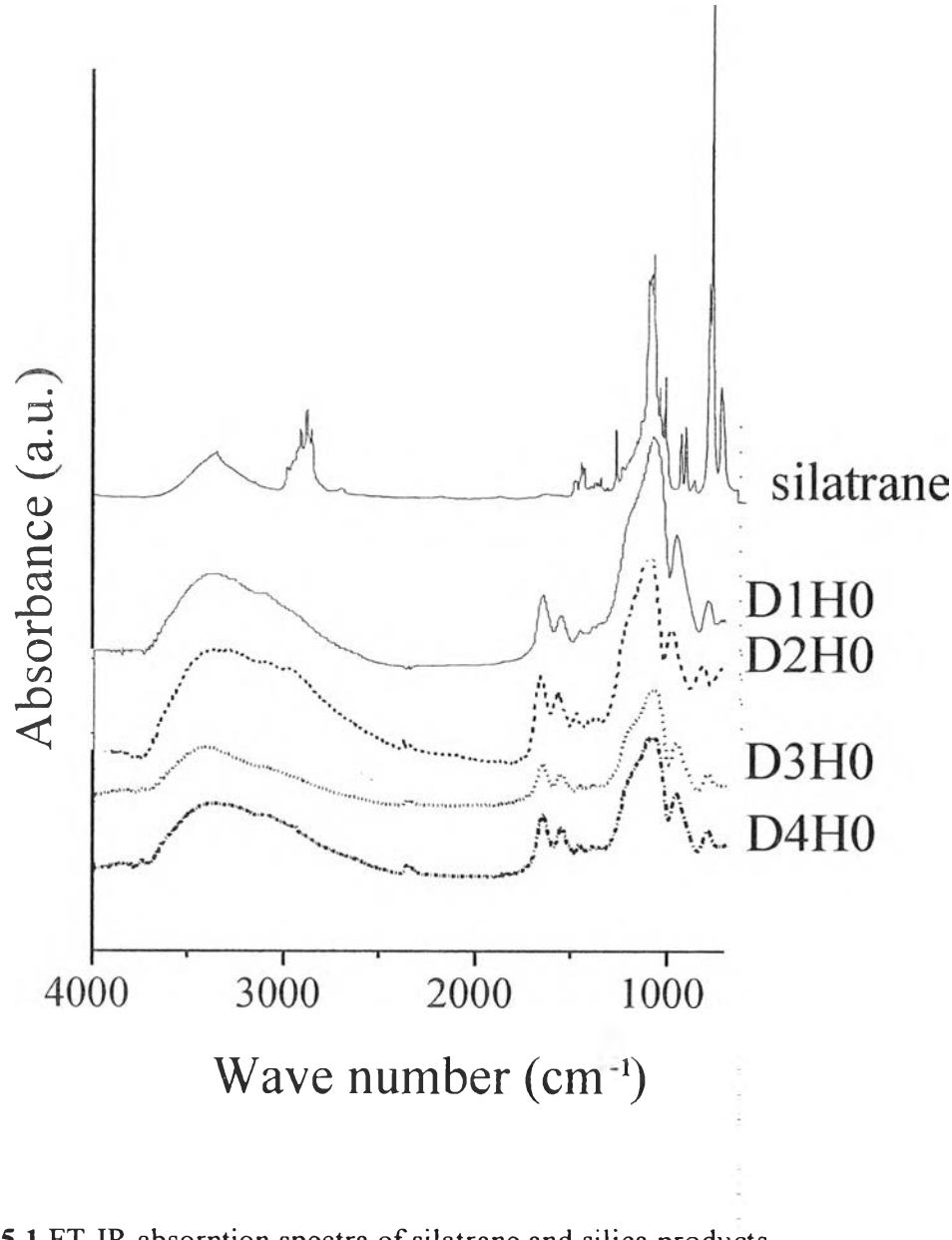

Figure 5.1 FT-IR absorption spectra of silatrane and silica products.

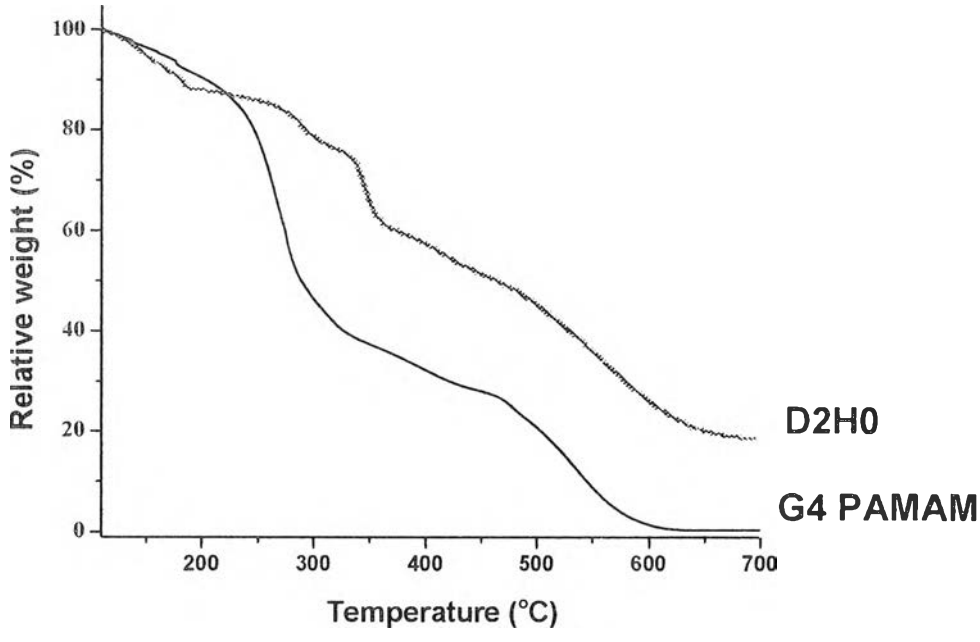

Figure 5.2 TGA curves of D2H0 and G4 PAMAM dendrimer.

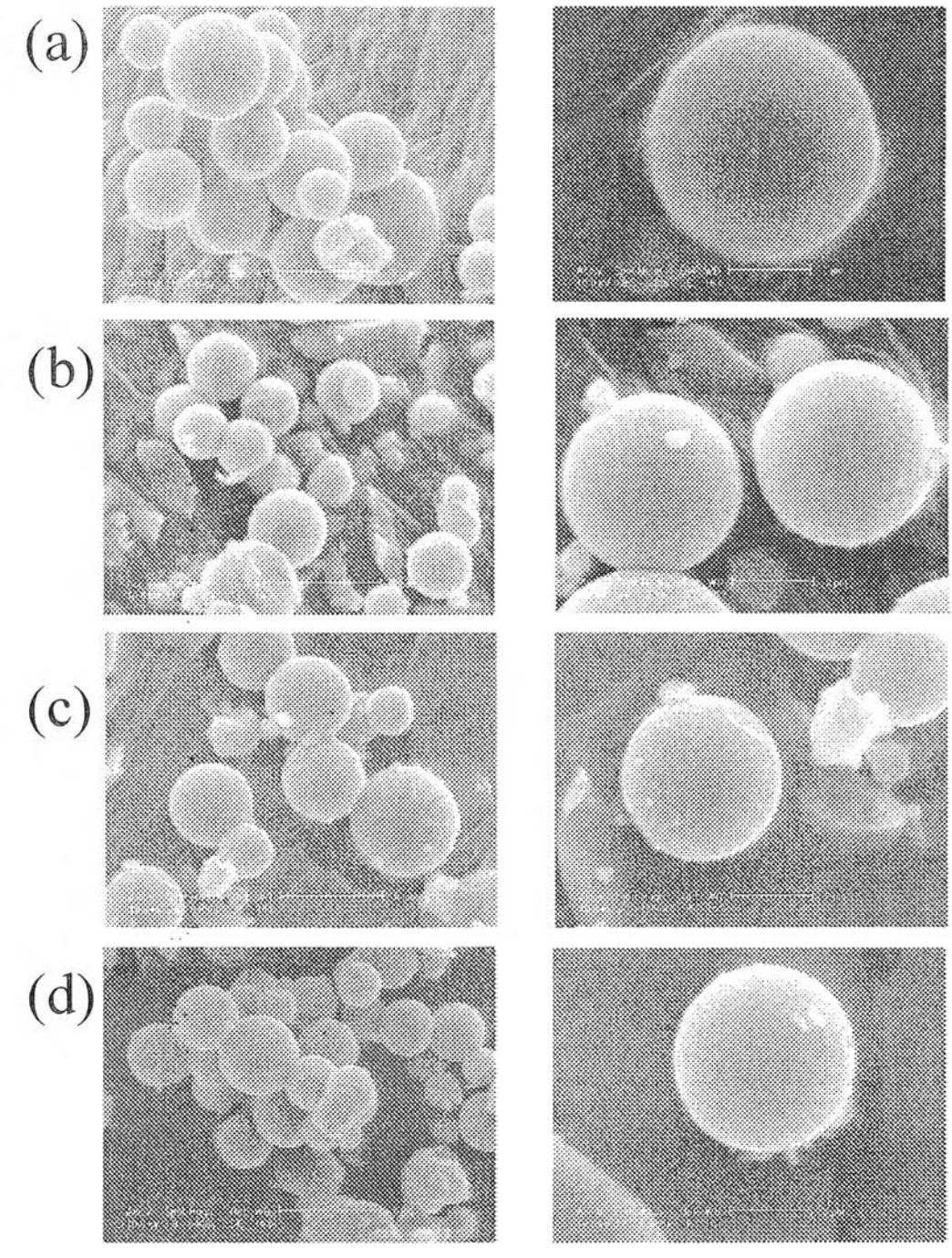

Figure 5.3 SEM images of DnH0. (a) D1H0, (b) D2H0, (c) D3H0, (d) D4H0.

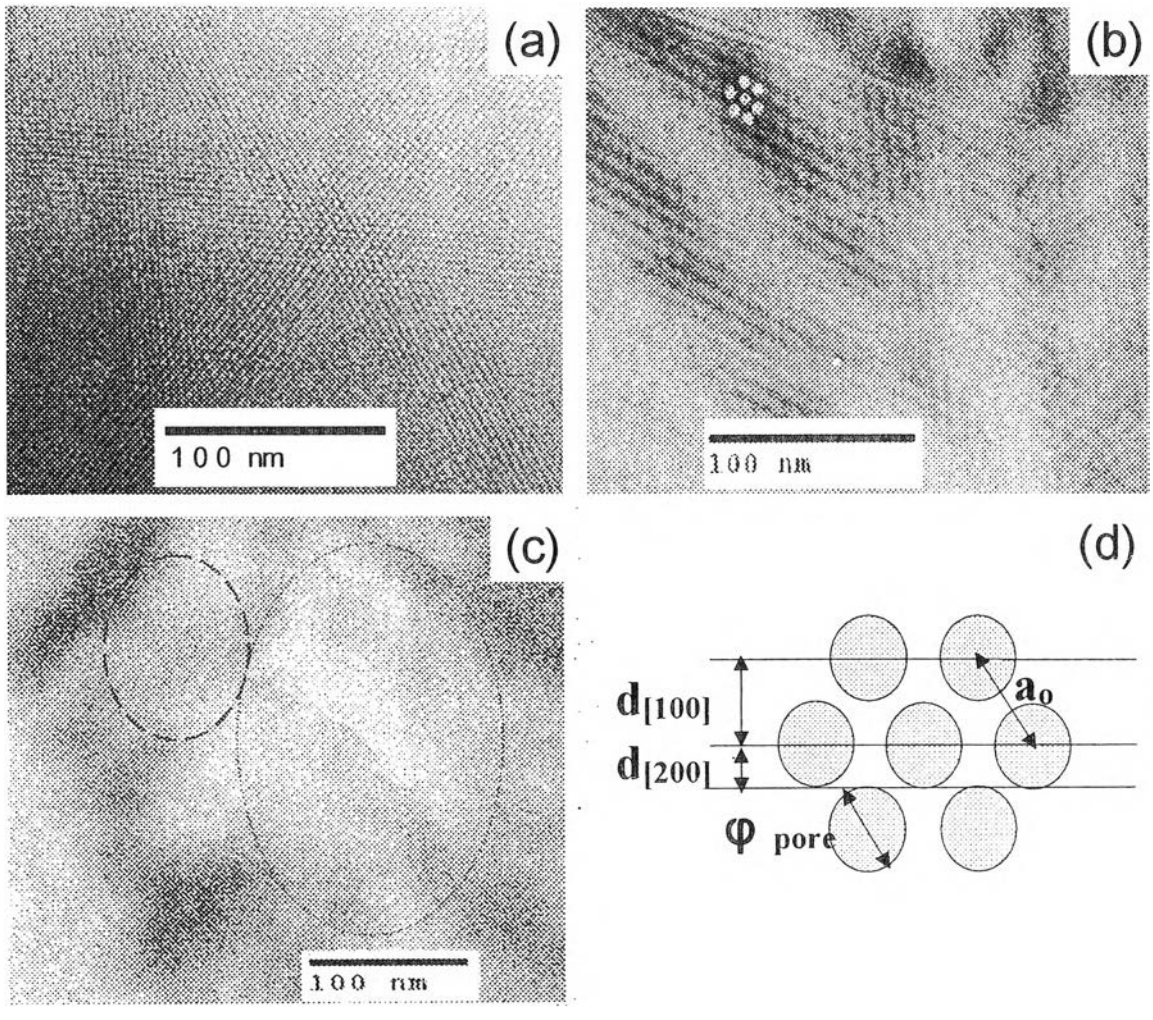

Figure 5.4 TEM images of silica products (a)-(c) and an illustration of hexagonal packing and indices (d). (a) D4H0 (array S), (b) D3H10 (array L), (c) D4H0 (array S and L).

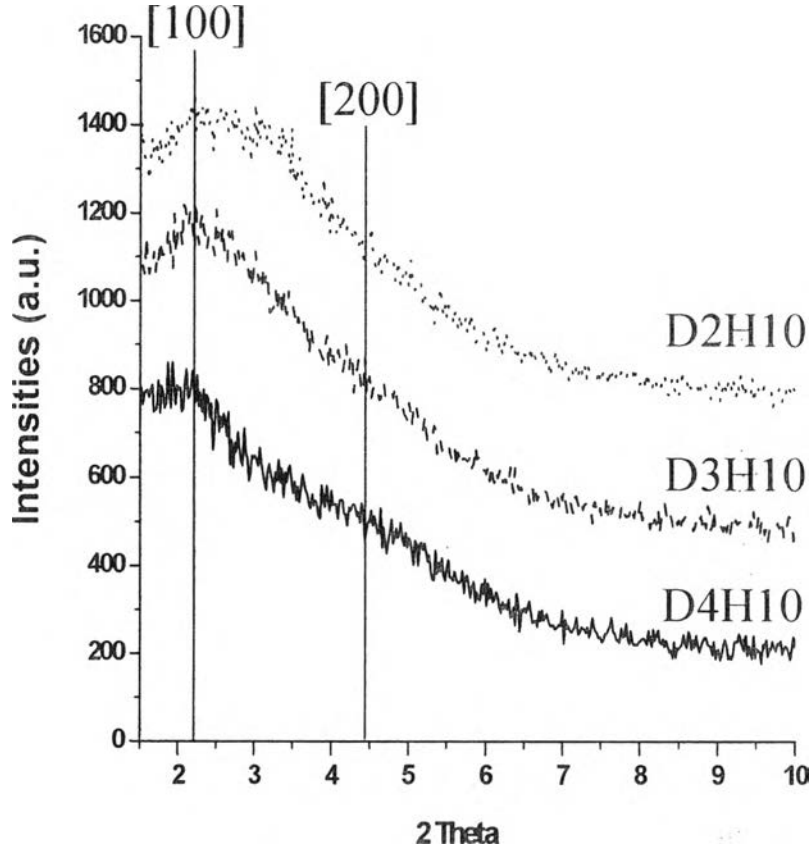

Figure 5.5 XRD data of silica products.

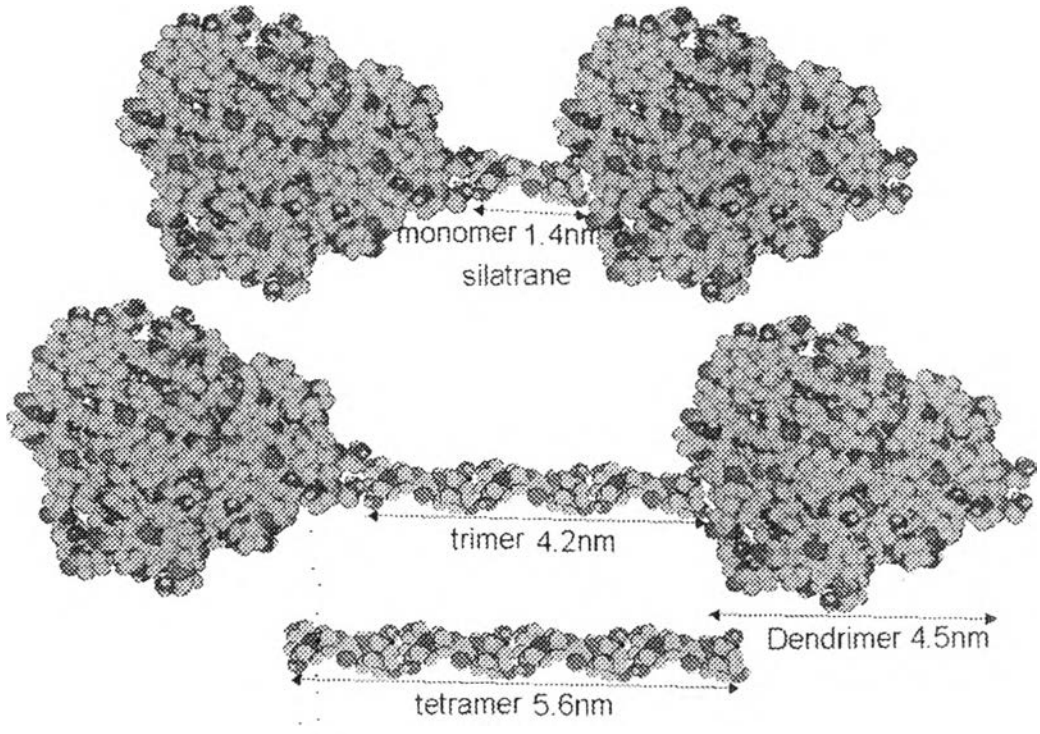

Figure 5.6 CPK models of silatrane, silatrane oligomers, and G4 PAMAM dendrimer.